Generalized Minimum-Time Follow-up Approaches Applied to Tasking Electro-Optical Sensor Tasking

Timothy S. Murphy, Marcus J. Holzinger
The Guggenheim School of Aerospace Engineering, Georgia Institute of Technology

This work proposes a methodology for tasking of sensors to search an area of state space for a particular object, group of objects, or class of objects. This work creates a general unified mathematical framework for analyzing reacquisition, search, scheduling, and custody operations. In particular, this work looks at searching for unknown space object(s) with prior knowledge in the form of a set, which can be defined via an uncorrelated track, region of state space, or a variety of other methods. The follow-up tasking can occur from a variable location and time, which often requires searching a large region of the sky. This work analyzes the area of a search region over time to inform a time optimal search method. Simulation work looks at analyzing search regions relative to a particular sensor, and testing a tasking algorithm to search through the region. The tasking algorithm is also validated on a reacquisition problem with a telescope system at Georgia Tech.

I. Introduction

A. Background

The space domain awareness (SDA) mission continues to require increased efficiency for catalog upkeep and catalog expansion [1]. As the Space Surveillance Network expands, increased numbers of sensors will become available, allowing for more complex operations. Additional pushes have been made to look for alternative data collection via either dedicated space based sensors or unconventional optical sensors in space such as star trackers [2]. This work in particular is derived in a general framework for any sensor type, then specialized to the electro-optical sensor (EOS), that is, cameras. In many cases, these sensors will make large numbers of detections on space objects (SO), some of which may appear with a unique trajectory and photometric signature that warrants follow-up. As of now, there is limited work on how to act on this information without collocated sensors and short follow up times.

A variety of sensor tasking strategies have been proposed, which typically look at the tasking problem in terms of catalog upkeep [3, 4, 5, 6]. These techniques tend to look at the strategic tasking problem, that is, how to use a network of sensor to look at a catelog of objects. These methods often don't account for region shape, and are limited to objects with well posed prior information. This work looks to analyze the tactical tasking problem, that is, given a prior and a sensor, how should the sensor look through the prior? In particular, this work extends a particle based search strategy proposed by Hobson [7]. Long term, this work will be combined with modern models for prior information in space objects, namely sequential Bayesian filters [8, 9].

This paper looks at how to search through a set of orbits. For example, an uncorrelated track (UCT), obtained from an EOS, can be used to define an admissible region [10, 11]. This set of orbits can be propagated and projected into the field of regard of new sensors at a new time. In general, this region can be much larger than the field of view of a sensor, and requires multiple observations [12]. Existing methods are based on a greedy maximum probability observation technique, which looks at observing the densest region of probability [13]. The sets used in this framework can be defined through reachability [17], hypothesized regions of state space, or any other way. The idea behind this work is that, if a prior can be formulated as a set, this work can be used to analyze that set.

The biggest problems facing this technique are how to choose an optimal trajectory when performing a search, and what type of optimality is desirable. This paper argues that time optimality is the highest priority. Many SDA sensor systems have a problem of too many objects and not enough sensors, making time on high sensitivity sensors a priority. Furthermore, when searching a set of orbits, there is guaranteed definition of probability. If probability density information is available, a greedy maximum probability observation may take significantly more time if an object appears on the fringes of the PDF. Finally, an EOS can be prone to false detections; it is typically more wise to search the entire search set than to trust the first detection that is made. Therefore time-optimal tasking is pursued in this paper.

This optimization problem, then, is the covering salesman problem (CSP), a variation of the traveling salesman problem [14]. The CSP looks for the optimal path to take between a series of points such that every point, or a point within a limiting distance, is visited. The tasking problem outlined above has a further complication over the classic CSP, in that the points to be visited have dynamics, and typically spread out as time passes. This problem will in

general be NP-hard, and obtaining complete optimal solutions is difficult. This paper will therefore both attempt the time optimal optimization, but also develop tools that can efficiently analyze the search. Once an observation is made, there exist a variety of techniques for making correlation [15]. This problem is also relevant to allowing non-collocated EOS to observe a single object simultaneously for fast orbit determination [16]. This work looks at the feasibility of different hand-off techniques.

B. Broad Categories of Search

This paper provides a broad definition of search. Search is the process of looking for an object, or group of objects, which is thought to exist within a set of orbits, known as the search set. The set of orbits could be defined through a variety of methods. In a lost object scenario, the a priori PDF which takes into account conservative dynamics uncertainties, can have a search set defined directly by bounding the PDF. Compared to assuming a Gaussian distribution, this method is preferred on inherently unknown or difficult to quantify dynamics. Inherently set based methods, such as an admissible region, easily define a search set [11]. Objects which have performed an unknown maneuver can be used to define a set of orbits by providing a limiting bound on total fuel expenditure [17]. Object maneuver limits can also be applied to other anomalous events such as a satellite break up. Finally, a search set can be defined more broadly as a region of orbits where objects may exist for an object discovery type methods. Furthermore, this definition is not restricted to space objects; search for particular classes of asteroids, search in air or sea domains, and a variety of other problems all fit within this framework.

This paper acknowledges two categories in which the search described in this paper would be useful. The first is the problem of how to search an area of state space to maintain custody of objects in it. To protect a certain asset, it is useful to be able to assure that the set of intercept orbits does not contain a hostile threat. There are a variety of other ways to pose this problem, but the common theme is constantly searching a large set of orbits to find previously unknown objects.

The second type of search is to perform follow up on an object where its location is not entirely known. A prime example of this is the follow up on an object with a prior characterized by an admissible region. This can be broadened to searching for debris after a break up event, to search for an object that has maneuvered, and reacquisition of an catalog object with sufficiently large uncertainties. If the search region for this object is large, the search strategies may be similar to that of the custody problem, while for a small search region it becomes more feasible.

C. Methodology

The first requirement is an analytic formulation of the problem. An EOS tasking scheme will be thought of as a series of observations taken at a series of fixed angular coordinates, at a series of fixed time steps. These discrete task locations can consist of any number of observations taken at any locations in any order. Quantities like exposure time and number of observations taken at each location could be varied, as well as characteristics of the sensor, though this particular work fixes these quantities for simplicity. This paper will assume for simplicity that if a sensor looks in the direction of an object, the object is detected, or in other words, missed detections are not considered. As this work matures, a belief and plausibility filter will be incorporated into the search algorithm to better quantify missed detections and false detections [22].

An analysis on the area of a search set, through analysis of divergence, is presented. The rate of change of the area of a region can be calculated via a line integral over the boundary of the region, in the measurement space. This is then extended to higher order derivatives to enable the area of a region to be accurately predicted over a long period of time. A region of high divergence will grow quickly, increasing the total number of observations needed to observe it. The implication is, a time optimal algorithm will prioritize high divergence. This analysis first provides a method to analyze search sets relative to a particular sensor, giving estimates of search campaign length and search feasibility. Second, this method is used directly as a cost function in creating time optimal trajectories.

An optimization cost function is then proposed as a way to choose a trajectory. This work will look to minimize the amount of time spent searching for the object, while attempting to scan the entire search area defined by prior information. In previous work, a variation on simulated annealing [18] was tried with some success. Due to the high dimensional and non-convex search space, this optimization can be difficult to successfully implement. A second cost function which looks at maximizing how much the observed area grows at some time horizon is also shown. This cost function is suited for a finite time horizon control approach.

In order to test the tasking algorithm, and illustrate its performance behavior to the reader, two simulated test cases are presented. The first one looks at a same location handoff. An admissible region, formed from a short arc observation is propagated an hour into the future, and reacquisition is attempted. This test case shows off many of the strengths of the work in this paper. Second, a search set is defined to contain objects in geostationary transfer orbits

which will intersect a particular GEO slot over a given time interval. This search set and subsequent tasking simulation showcase the variety of scenarios these techniques can be applied to.

II. Theory: Search Regions

This section will introduce the concept of a search set, a set of orbits that a sensor or group of sensors must search through. Then a series of analytic tools with be presented for analyzing a search set and the projection of the search set into a measurement subspace. The intention is to provide insight into the nature of these sets and the implications on their searchability.

A. General Problem Framework

First this paper requires defining the general dynamics framework. Define $\mathcal{X}$ as the set of all states, which in practice could be position and velocity, or some alternative representation like orbit elements. Given a dynamic system,

$$\dot{\mathbf{x}} = \mathbf{f}(\mathbf{x}) \tag{1}$$

an object can be propagated forward in time via a flow function

$$\mathbf{x}(t_1) = \boldsymbol{\phi}(t_1; \mathbf{x}(t_0), t_0) \tag{2}$$

which simply propagates a state via the dynamics in Equation (1). This paper will consider the propagation of not just a single state, but a set, referred to as the search set. Consider a set of dynamic states, $\mathcal{S}(t_0) \subset \mathcal{X}$, which may be defined as a series of constraints $\{g_a(\mathbf{x})\}_{a=1}^{b}$

$$\mathcal{S} = \{\mathbf{x} \in \mathcal{X} : g_a(\mathbf{x}) \leq 0 \ \forall \ a\} \tag{3}$$

Because each element in this set is dynamic, the set can be propagated as

$$\mathcal{S}(t) = \boldsymbol{\phi}(t; \mathcal{S}(t_0), t_0) \tag{4}$$

Note that this region is time varying, according to orbital mechanics; the time notation will be dropped unless explicitly necessary.

The space in which this set exists, $\mathcal{X}$, is in effect a phase space representation. In accordance with Liouville's theorem, the measure, $|\cdot|$, a generalization of volume, of this set must stay constant under the given dynamics [19]. However, note that many of the sets used in this work are sub-dimensional manifolds in $\mathcal{X}$, and therefore have zero measure.

This paper requires analyzing orbits within the measurement space defined by a particular sensor, $\mathcal{H}_i$, where this space has dimension h. A state, $\mathbf{x}$, can be mapped to a measurement taken by a particular observer, $\mathbf{x}_d$, representing the subspace of the state determined by the measurement. This requires a measurement function, $\mathbf{h}_i$, which maps the full state space into the measurement subspace,

$$\mathbf{x_d} \in \mathcal{H}_i \tag{5}$$

$$\mathbf{h}_i : \mathcal{X} \to \mathcal{H}_i \tag{6}$$

The i subscript, which refers to which observer is being considered, will be dropped unless multiple observers are being explicitly used. In the case of inherent unobservability, there is also an unobservable subspace, so the state can be partitioned into two sub-components,

$$\mathbf{x} = [\mathbf{x_d}^T, \mathbf{x_u}^T]^T \tag{7}$$

$$\tag{8}$$

where $\mathbf{x_u}$ is part of a state unobserved by a particular observer, based on notation used in [11]. Similarly, a search set can be projected into the measurement space,

$$\mathcal{S}_d = \mathbf{h}(\mathcal{S}), \mathcal{S}_d \subseteq \mathcal{H} \tag{9}$$

Note that this mapping is a projection onto a subspace, so multiple elements of $\mathcal{S}$ may map to a single component of $\mathcal{S}_d$. The nominal evolution of both $\mathcal{S}$ and $\mathcal{S}_d$ are illustrated in Figure 1. Note that while $|\mathcal{S}(t_0)| = |\mathcal{S}(t)|$ in accordance with Louisville's Theorem, in general $|\mathcal{S}_d(t_0)| \neq |\mathcal{S}_d(t)|$ as they exist in a subspace of the phase space.

An observation can be modeled as a subset of the search set. A sensor is tasked to observe a particular region of the measurement space, at a particular time step, represented by $\mathcal{O}(t_k) \subset \mathcal{H}$.

A requirement for successful search is that every part of $\mathcal{S}$ is observed. At each time step, a section of the measurement space is observed through $\mathcal{O}$. Given a projected search space at time step k, $\mathcal{S}_d(t_k)$, the observed part of the space is $\mathcal{S}_d(t_k) \cap \mathcal{O}(t_k)$, while the unobserved part is $\mathcal{S}_d(t_k) \setminus \mathcal{O}(t_k)$. This paper defines $\mathcal{S}(t_k)$ as the search space at time step k, or in other words, the set of orbits that need to be observed. Once a part of the set has been observed it no longer needs to be observed and should therefore no longer be part of the search space. Therefore, at each timestep, the search space is redefined as

$$\mathcal{S}(t_k^+) = \{\mathbf{x} \in \mathcal{S}(t_k^-) : \mathbf{h}(\mathbf{x}) \notin \mathcal{O}(t_k)\} \tag{10}$$

where t_k^- and t_k^+ are timestep k before and after the update. Note that the removal of $\mathcal{O}(t_k)$ from $\mathcal{S}(k-)$ does not necessarily imply that an object does not exist in $\mathcal{S}_d(t_k) \cap \mathcal{O}$, but that that part of the space has been searched. Missed detections may lead to such a situation. The optimal tasking problem then is constrained to, in some optimal manner, drive the size of the search space, $|\mathcal{S}(t_k)|$, to zero.

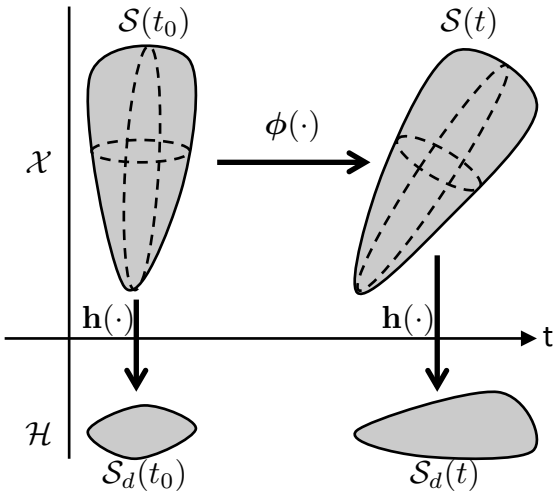

Figure 1. The search space evolves over time, in both $\mathcal{X}$ and $\mathcal{H}$

B. Search Region Area

The area of a search region at a given time is a useful quantity in the analysis of search regions. However, there are several different measures of area, when dealing with projections of high dimensional sets. This paper will analyze the spatial area of a projected search region, $|\mathcal{S}|_{\mathcal{H}}$, as the spatial area of the set $\mathcal{S}$ when projected into the measurement space. Note that the spatial area is not the full measure of the set, as it measures the projected set and even then does not include the velocity states which often exist in the measurement space. The spatial area, $|\cdot|_{\mathcal{H}}$, is useful for quantifying the area a sensor can measure. In particular, the amount of a search space an optical sensor can measure is defined by the field of view of the sensor. For ease of notation, this area will from now on be represented as

$$A_{\mathbf{h}}(\mathcal{S}) = |\mathcal{S}|_{\mathcal{H}} \tag{11}$$

This area, then, is a function of the search set which is itself a function of time, $A_{\mathbf{h}}(\mathcal{S}(t))$. However, a set of orbits doesn't necessarily have a clean analytic definition, and the propagation the the set over time has no analytic solution, so this area is not always well defined. In the worst case scenario, a set of orbits can be brute force represented with particles which can be used to approximate the area.

The area of this search region has implications on the search ability of a set. In most realistic scenarios, different velocities within a search set cause the set to expand spatially. Conversely, an observer will, with each observation, reduce the remaining area that must be searched. A successful search requires the observations to reduce the search area faster than the expansion is causing the area to rise.

C. Search Area and Divergence

What this section looks to determine is both the growth rate of a search region as seen by a particular sensor, and the local regions of expansion and contraction. The main motivation for this section is the fact that the search region over time is not analytically known. Assume that an observer, located at $\mathbf{o}(t_o)$, wants to take an observation in this search space at time t_o. First, the search set must be propagated to the appropriate time, via Equation (4). Next, the search set must be projected into the field of regard of a sensor, through some measurement function $\mathbf{h}$,

$$\mathbf{x}_d = \mathbf{h}(\mathbf{x}) \tag{12}$$

$$\mathcal{S}_d = \{\mathbf{x}_d : \mathbf{x}_d = \mathbf{h}(\mathbf{x}), \mathbf{x} \in \mathcal{S}\}. \tag{13}$$

The function $\mathbf{h}$ maps to $\mathbf{x}_d$, the component an observer can measure.

A few problems involved in calculations can be side stepped using the divergence theorem. To review, the divergence theorem states that for a vector field, $\mathbf{F}$, defined over a region $\mathcal{S}$, with boundary $\partial\mathcal{S}$,

$$\int_{\mathcal{S}} \nabla \cdot \mathbf{F} \mathrm{d}V = \oint_{\partial\mathcal{S}} (\mathbf{F} \cdot \hat{\mathbf{n}}) \mathrm{d}S \tag{14}$$

where ∇ is the vector of derivatives with respect to $\mathbf{x}_d$. By setting $\mathbf{F}$ equal to $\mathbf{x}_d$, this integral implies that the area of a particular region of state space can be calculated as the total integral

$$A_{\mathbf{h}}(\mathcal{S}) = \int_{\mathcal{S}_d} \mathrm{d}V = \frac{1}{\dim} \int_{\mathcal{S}_d} \nabla \cdot \mathbf{x}_d \mathrm{d}V = \frac{1}{\dim} \oint_{\partial\mathcal{S}_d} (\mathbf{x}_d \cdot \hat{\mathbf{n}}) \mathrm{d}S \tag{15}$$

where dim is the dimensionality of the space, used to normalize $\nabla \cdot \mathbf{x}_d$. The lower dimensional version of this equation is known as Green's theorem and will be discussed in the follow section.

Note that the bounds and differentials on this integral are functions of time, so to analyze the immediate expansion or contraction of a search region, the Leibniz integral rule can be used to take the first derivative as

$$\begin{aligned} \frac{\mathrm{d}}{\mathrm{d}t} A_{\mathbf{h}}(\mathcal{S}) &= \frac{1}{\dim} \frac{\mathrm{d}}{\mathrm{d}t} \int_{\mathcal{S}_d} \nabla \cdot \mathbf{x}_d \mathrm{d}V \\ &= \frac{1}{\dim} \int_{\mathcal{S}_d} \frac{\partial}{\partial t} (\nabla \cdot \mathbf{x}_d) \mathrm{d}V + \frac{1}{\dim} \oint_{\partial\mathcal{S}_d} (\nabla \cdot \mathbf{x}_d)(\dot{\mathbf{x}}_d \cdot \hat{\mathbf{n}}) \mathrm{d}S \\ &= \oint_{\partial\mathcal{S}_d} (\dot{\mathbf{x}}_d \cdot \hat{\mathbf{n}}) \mathrm{d}S. \end{aligned} \tag{16}$$

This is an easy to calculate value which only involves the velocity at the boundary of the region. For further intuition, the expansion is mathematically captured by the divergence of velocity vector field,

$$\mathrm{div}(\dot{\mathbf{x}_d}) = \nabla_{\mathbf{x}_d} \cdot \dot{\mathbf{x}_d} \tag{17}$$

which when combined with Equation (14), yields

$$\oint_{\partial\mathcal{S}_d} (\dot{\mathbf{x}}_d \cdot \hat{\mathbf{n}}) \mathrm{d}S = \int_{\mathcal{S}_d} \nabla \cdot \dot{\mathbf{x}}_d \mathrm{d}V. \tag{18}$$

The implication of this equation is that the contribution to the expansion (or contraction) of the region at any particular point is due solely to the divergence of the velocity vector field. Taking the derivative of Equation (16)

$$\begin{aligned} \frac{\mathrm{d}}{\mathrm{d}t} \oint_{\partial\mathcal{S}_d} (\dot{\mathbf{x}}_d \cdot \hat{\mathbf{n}}) \mathrm{d}S &= \oint_{\partial\mathcal{S}_d} \frac{\partial}{\partial t} (\dot{\mathbf{x}}_d \cdot \hat{\mathbf{n}} \mathrm{d}S) \\ &= \oint_{\partial\mathcal{S}_d} \left(\ddot{\mathbf{x}}_d \cdot \hat{\mathbf{n}} + \dot{\mathbf{x}}_d \cdot \frac{\partial \dot{\mathbf{x}}_d}{\partial \mathbf{x}_d} \cdot \hat{\mathbf{n}} \right) \mathrm{d}S \end{aligned} \tag{19}$$

which requires calculation of the partials of the velocity vector field with respect to position. Further derivatives are possible as well which are included in an appendix at the end of this paper.

Because a search region of arbitrary dimension and shape is being projected through a non-injective function, multiple orbits with multiple velocities could all project to a single $\mathbf{x}_d$. Even if $\dim(\mathcal{S}) = \dim(\mathcal{S}_d)$, the manifold of $\mathcal{S}$ might be folded in such a way that two or more parts of the original manifold map to the same part of $\dim(\mathcal{S}_d)$. The

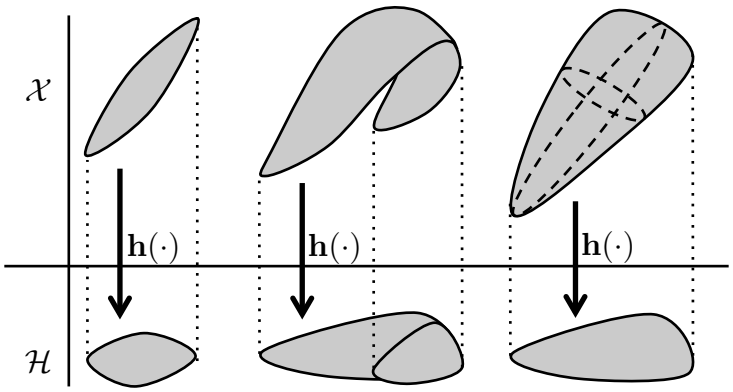

Figure 2. Cases manifold projection for one-to-one, discrete-to-one, and continuum-to-one

vector field is then ill-defined. Therefore, this work will consider the 3 possible cases; the first is when the projection is one to one, the second is when the projection is a discrete number of points to one (folding), and the third is when a continuum of points in the original manifold map to a single point in the projected manifold. These three cases are illustrated in Figure 2. For the one-to-one case, Equation (16) can be calculated directly, as can future derivatives. For the discrete-to-one case, $\dot{\mathbf{x}}_d$ will have multiple values at a single $\mathbf{x}_d$. Equation (16) will have several disparate values on each level of the original manifold. For any analytic purposes, these sub manifolds have completely unique properties and need no special treatment.

If the projection is such that a continuum of points are mapped to a single point in the measurement space, a continuum of velocity vector fields are defined over the search set. Calculating area and divergence becomes difficult as there are multiple values for divergence at any given point. This paper proposes defining an upper bound to the area rate based on maximum possible line integral from the vector fields. Given a series of vector fields, define the set of $\dot{\mathbf{x}}_d$ defined at a particular $\mathbf{x}_d$,

$$S_{\dot{\mathbf{x}}_d}(\mathbf{x}_d) = \left\{ \dot{\mathbf{x}}_d = \frac{\mathrm{d}}{\mathrm{d}t}(\mathbf{h}(\mathbf{x})) : \mathbf{x}_d = \mathbf{h}(\mathbf{x}) \right\} \tag{20}$$

This set definition now enables the following inequality,

$$\oint_{\partial \mathcal{S}_o} \dot{\mathbf{x}}_d \cdot \hat{\mathbf{n}} \mathrm{d}S \leq \oint_{\partial \mathcal{S}_o} \sup_{\mathbf{y} \in S_{\dot{\mathbf{x}}_d}} (\mathbf{y} \cdot \hat{\mathbf{n}}) \, \mathrm{d}S \tag{21}$$

where the supremum chooses the velocity with the largest outward orthogonal component at any given point along the boundary. This integral will be larger than any other piece-wise combination of vector fields. To understand the implication of this inequality, consider

$$\mathbf{x}_1, \mathbf{x}_2 \in \mathcal{S} : \mathbf{h}(\mathbf{x}_1) = \mathbf{h}(\mathbf{x}_2) = \mathbf{x}_d \in \partial \mathcal{S}_d. \tag{22}$$

Now, it is easy to show

$$\dot{\mathbf{x}}_{d,1}(t) \cdot \hat{\mathbf{n}} > \dot{\mathbf{x}}_{d,2}(t) \cdot \hat{\mathbf{n}} \rightarrow \mathbf{x}_{d,2}(t + \delta t) \notin \partial \mathcal{S}_d \tag{23}$$

because the boundary $\partial \mathcal{S}_d$ must be moving outward at at least a rate of $\dot{\mathbf{x}}_{d,1} \cdot \hat{\mathbf{n}}$. In other words, if $\mathcal{S}_d$ has a continuum of velocity vector fields, the internal motion still does not effect the growth of the region, and the expansion at the boundary is fully described by $\sup_{\mathbf{y} \in S_{\dot{\mathbf{x}}_d}} (\mathbf{y} \cdot \hat{\mathbf{n}})$.

Finally, it is worth considering the behavior of partitions of a search set. The search space $\mathcal{S}_d$ can be partitioned into m sub regions,

$$\mathcal{S}_d = \bigcup^{m} \mathcal{S}_d^i \tag{24}$$

$$\emptyset = \mathcal{S}_d^a \cap \mathcal{S}_d^b \ \forall \ a \neq b \tag{25}$$

where $\mathcal{S}_d^i$ are the non-overlapping partitions. The area over time, and area growth, can be calculated for each partition to give insight into local areas of growth within the search space. Note that unless the manifold mapping into the search space is one-to-one, non-overlapping partitions in $\mathcal{H}$ may overlap in the future.

D. Admissible Region based Search Area

This section focuses on how to applying the previous analysis to the primary test case of this paper, follow up on an admissible region by an optical observer. Consider an admissible region, $\mathcal{AR}$, defined at some previous time t_0. Assume that an optical observer, located at $\mathbf{o}(t)$, wants to search $\mathcal{AR}$ at time t_f.

$$\mathbf{x}_d = [\alpha, \delta]^T = \mathbf{h}(\mathbf{x}; \mathbf{o}) \tag{26}$$

$$\mathcal{S}_d = \{[\alpha, \delta]^T : [\alpha, \delta]^T = \mathbf{h}\left(\phi(t_f; \mathbf{x}, t_0); \mathbf{o}(t_f)\right), \mathbf{x} \in \mathcal{AR}\}. \tag{27}$$

The divergence for this optical sensor is

$$\text{div}(\mathbf{x}_d) = \frac{\mathrm{d}\dot{\alpha}}{\mathrm{d}\alpha} + \frac{\mathrm{d}\dot{\delta}}{\mathrm{d}\delta}. \tag{28}$$

The area can then be calculated as

$$A_{\mathbf{h}}(\mathcal{S}) = \frac{1}{2}\oint_{\partial\mathcal{S}_d} (\mathbf{x}_d \cdot \hat{\mathbf{n}})\mathrm{d}S = \frac{1}{2}\oint_{\partial\mathcal{S}_d} -\delta\cos(\delta)\mathrm{d}\alpha + \alpha\mathrm{d}\delta \tag{29}$$

where the signs and arrangement of α and δ account for the normal vector. The area rate of change is

$$\frac{\mathrm{d}}{\mathrm{d}t}(A_{\mathbf{h}}(\mathcal{S})) = \oint_{\partial\mathcal{S}_d} -\dot{\delta}\cos(\delta)\mathrm{d}\alpha + \dot{\alpha}\mathrm{d}\delta\mathrm{d}S \tag{30}$$

Note that any occurrence of $\mathrm{d}\alpha$ has an additional factor of $\cos(\delta)$. This is because a differential in angular space such as $\mathrm{d}S$ or $\mathrm{d}A$ must account for the curved nature of the angular space. This also implies that all angles must be represented in radians, and the area being calculated is in steradians. These may also be difficult or impossible to calculate near the singularities at $\delta = \pm\pi/2$.

The higher order derivatives of $A_{\mathbf{h}}$ exist and can be calculated. An infinite Taylor series can be used to approximate the area over time to very high accuracy. The calculations are analytic and are often relatively easy to calculate, compared to particle propagation. It can be assumed that sufficient accuracy is achievable by increasing the number of terms in the Taylor series approximation.

The admissible region from an optical observer is a 2 dimensional manifold of orbits. Any search set will therefore be either entirely one-to-one or have some folding that causes multiple orbits to map to a single α and δ pair. Qualitatively, there is no guarantee that folding will not occur, but over short periods of time after the inception of $\mathcal{AR}$, folding tends to not occur. The structure of $\mathcal{AR}$ makes the analysis on partitioning particularly powerful; because $\mathcal{AR}$ is a continuously defined region, partitioned regions will not overlap outside of folding. Figure 3 shows the divergence changing over a region.

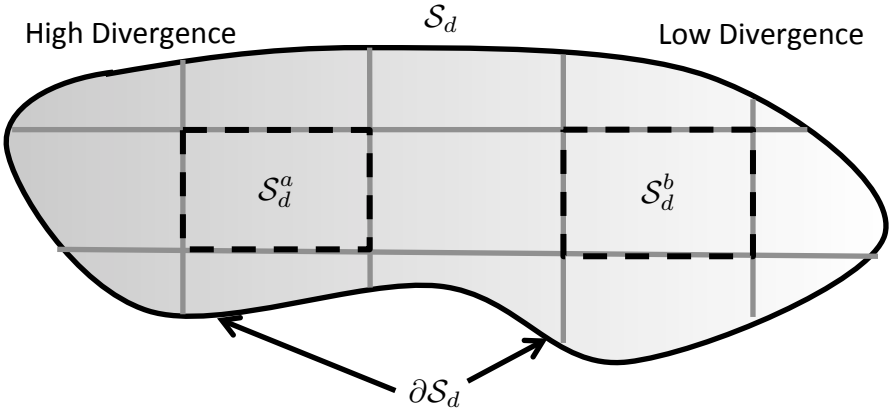

Figure 3. Divergence of $\dot{\alpha}$ and $\dot{\delta}$ as they vary with α and δ

If no folding occurs for a 2 dimensional manifold, the original boundary of the manifold will be associated with the projected boundary. When considering an admissible region, the projected boundary of the region then often corresponds to the boundary of $\mathcal{AR}$ in the original space.

Equation (19) requires calculating $\frac{\partial\dot{\mathbf{x}}_d}{\partial\mathbf{x}_d}(t)$. This quantity must be calculated along a the manifold created by the propagated admissible region, $\mathcal{S}_d(t)$. This manifold, at a particular time t, does not have a closed form definition.

Instead the derivative must be tied back to the original definition of the manifold, that is, the original admissible region. The variations of a location in $\mathcal{H}$ with respect to admissible region coordinates is

$$\begin{aligned}\frac{\partial \mathbf{x}_d(t)}{\partial \mathbf{x}_u(t_0)} &= \frac{\partial \mathbf{x}_d(t)}{\partial \mathbf{x}(t)}\frac{\partial \mathbf{x}(t)}{\partial \mathbf{x}(t_0)}\frac{\partial \mathbf{x}(t_0)}{\partial \mathbf{x}_u(t_0)} \\ &= \frac{\partial \mathbf{x}_d(t)}{\partial \mathbf{x}(t)}\Phi(t, t_0; \mathbf{x}(t_0))\frac{\partial \mathbf{x}(t_0)}{\partial \mathbf{x}_u(t_0)}\end{aligned} \tag{31}$$

where $\frac{\partial \mathbf{x}_d(t)}{\partial \mathbf{x}(t)}$ is the Jacobian of the measurement function, $\mathbf{h}$, and Φ is the state transition matrix. Similarly,

$$\begin{aligned}\frac{\partial \dot{\mathbf{x}}_d(t)}{\partial \mathbf{x}_u(t_0)} &= \frac{\partial \dot{\mathbf{x}}_d(t)}{\partial \mathbf{x}(t)}\frac{\partial \mathbf{x}(t)}{\partial \mathbf{x}(t_0)}\frac{\partial \mathbf{x}(t_0)}{\partial \mathbf{x}_u(t_0)} \\ &= \frac{\partial \dot{\mathbf{x}}_d(t)}{\partial \mathbf{x}(t)}\Phi(t, t_0; \mathbf{x}(t_0))\frac{\partial \mathbf{x}(t_0)}{\partial \mathbf{x}_u(t_0)}\end{aligned} \tag{32}$$

where, similarly, $\frac{\partial \dot{\mathbf{x}}_d(t)}{\partial \mathbf{x}(t)}$ is the Jacobian of the derivative of the measurement function. Then the quantity we are after is

$$\frac{\partial \dot{\mathbf{x}}_d(t)}{\partial \mathbf{x}_d(t)} = \frac{\partial \dot{\mathbf{x}}_d(t)}{\partial \mathbf{x}_u(t_0)}\left(\frac{\partial \mathbf{x}_d(t)}{\partial \mathbf{x}_u(t_0)}\right)^{-1}. \tag{33}$$

Note that although this definition requires a matrix inverse, and the final matrix being inverted is a two by two which is easy to calculate. The above calculation does not require a fine understanding of the manifold to calculate; instead for a particular point in the sky, the exact point in the admissible region is needed. The given $\rho, \dot{\rho}$ pair defines an orbit, which defines all the inputs to EQ (33). The same process as above can be used to calculated higher order derivatives, by replacing $\dot{\mathbf{x}}_d(t)$ with $\ddot{\mathbf{x}}_d(t)$.

The matrix in the above inverse is not guaranteed to be full rank. Qualitatively, the inverse not existing refers to the case where a small change in $\rho, \dot{\rho}$ provides no change in α, δ. The only case where moving along this two dimensional manifold provide no change in the measurement space is when the manifold (in $\mathcal{X}$) is directly orthogonal to the measurement subspace, $\mathcal{H}$. This case can happen in certain special cases, for example when $t = t_0$. More importantly, when folding is occurring in the measurement space, this undefined inverse will occur exactly along the fold. This fact is both good and bad; this calculation provides a useful way of predicting when a manifold is folding, but makes the area acceleration undefined along that boundary.

E. Analysis of Search Set

This section focuses on the type of analysis which is easily accessible for a region. As the search set is searched by an observer, the search set itself is reduced in size according to Equation (10). It is critical to understand that, even though a search set is reduced each time an observation is taken, there is no guarentee that a full search is possible with a given sensor. Given a particular sensor, $\mathbf{o}$, over every integration, t_I, at time t_k an known area of the sky can be observed, $\mathcal{O}_o(\mathbf{u}(t_k))$. Then the total change in search region area can be calculated at each time step as,

$$A_{\mathbf{h}}(t_k) = \sum_{i=0}^{\infty}\frac{\mathrm{d}^i}{\mathrm{d}^i t}A_{\mathbf{h}}(t_0)\frac{(t_k - t_0)^i}{i!} - \left|\bigcup_{i=0}^{k}\phi(t_k; \mathcal{S}_d(t_i) \cap \mathcal{O}_{d,i}(t_i), t_i)\right|_{\mathbf{h}} \tag{34}$$

which can easily be show through a Taylor series expansion. Note that this equation is explicitly dependent on the proposed search strategy, which will be modeled as a control input $\mathbf{U}$. Assuming the higher order terms are small, the requirement for a successful search is then

$$A_{\mathbf{h}}(t_k) + \frac{\mathrm{d}}{\mathrm{d}t_k}A_{\mathbf{h}}(t_k)(\Delta t) \leq |\mathcal{S}(t_k) \cap \mathcal{O}_d(t_k)|_{\mathbf{h}} \tag{35}$$

A simpler way to see this is, if in general $|\mathcal{S}_o(t(t_k))| \geq |\mathcal{S}_o(t_{k-1})|$, the search problem does not close, while if $|\mathcal{S}_o(t(t_k))| < |\mathcal{S}_o(t_{k-1})|$ the problem closes. This provides a simple and efficient calculation for evaluating whether a search region is searchable. Furthermore, the amount the area changes each time step provides insight into approximately how long a search should take. This analysis is predicated on what is effectively a linearization on the expansion rate of the search region; if $\frac{\mathrm{d}}{\mathrm{d}t}|\mathcal{S}_o(t)|$ is not approximately constant over the interval $t(0)$ to $t(t_k)$, then

Equation (34) does not hold. Orbit dynamics are non-linear are therefore the true solution can diverge from this approximation. As shown in Equation (19), the acceleration and other higher order terms of $A_{\mathbf{h}}$ are calculable, but require more complicated derivatives which may be difficult to calculate, depending on the way $\mathcal{S}$ is defined.

The partition divergence calculation gives a tool for defining short term high priority search areas. Over a lower divergence region, a region of higher divergence, given equal time, will expand into a larger, harder to search area. For example, in Figure 3, the region of high divergence on the left should be prioritized over the region of low divergence on the right.

Equation (34) has an infinite Taylor series expansion in it, implying a quantity that is practically impossible to calculate. Instead this expansion will need to be taken out to "enough" terms to guarantee sufficiently small errors. This can be done by defining both a time horizon, t_f, and a relative tolerance, ϵ_{rel}. Then the required N terms for an approximation out to a certain time horizon satisfies

$$\epsilon_{rel} > \sum_{i=0}^{N} \frac{\mathrm{d}^i}{\mathrm{d}^i t} A_{\mathbf{h}}(t_0) \frac{(t_f - t_0)^i}{i!} - \sum_{i=0}^{N-1} \frac{\mathrm{d}^i}{\mathrm{d}^i t} A_{\mathbf{h}}(t_0) \frac{(t_f - t_0)^i}{i!} = \frac{\mathrm{d}^N}{\mathrm{d}^N t} A_{\mathbf{h}}(t_0) \frac{(t_f - t_0)^N}{N!}. \tag{36}$$

It should be noted that the divergence method is probability distribution function (PDF) agnostic. When operating a pure set or a PDF whose effective boundaries are used to define a set, the method gives the same result. This is particularly relevant to admissible region theory, where a set is used to define a PDF. Divergence methods will operate identically on either representation of the admissible region, avoiding analytic confusion.

Search regions can become sufficiently large that a region extends out of the field of regard on an EOS. This may even extend to a ring of orbits around earth, or all of the unit sphere, $\mathbf{S}(2)$. In these cases, the total region divergence may no longer be a useful measure, but divergence of partitions is very much still a useful measure.

F. Reachability Considerations

Consider a search set, $\mathcal{S}(t_0) \subset \mathcal{X}$, as a set of initial conditions for an orbit. These orbits have well defined dynamics, and can therefore define a control problem. In this framework, the set at a future time step, $\mathcal{S}(t)$, can be written in terms of a reachability problem

$$\mathcal{S}(t) = \mathcal{R}(t, t_0, \mathbf{u}_{max}; \mathcal{S}(t_0)) \tag{37}$$

where $\mathcal{R}$ is the reachable set of orbits at time t, based on the initial condition set, $\mathcal{S}(t_0)$, and the maximum control effort $\mathbf{u}_{max}$. The problem discussed in above sections can then be cast as a reachability problem, where the search set at a given time step is the reachable set based on the initial condition set, $\mathcal{S}(t_0)$, and a maximum control effort of $\mathbf{u}_{max} = \mathbf{0}$.

This generalization allows the theoretical framework in this paper to incorporate unknown control effort. Using any in a variety of control distance analysis frameworks [17], a reachability set can be calculated and used as the search set. In general, $\mathcal{R}$ is not a manifold but rather full dimension subset of $\mathcal{X}$. Like $\mathcal{S}$ in sections above, $\mathcal{R}$ can be amended with constraints to make the search set more manageable. Calculation of the derivatives of $A_{\mathbf{h}}$ are based on an uncontrolled trajectory. Therefore the search set $\mathcal{S}_d$ grows faster than what is predicted by the search area divergence calculations. The analytic implications of this are not explored further in this paper.

III. Theory: Optimal Search

A. Search on an Admissible Region with an Optical Sensor

For this paper, the search region elements are assumed to be orbits consisting of position and velocity at a given time, $\mathbf{x}(t) = [\mathbf{r}^T(t), \mathbf{v}^T(t)]^T \in \mathbb{R}^6$. This search region could be defined in a variety of ways, including from an admissible region, by defining a region of state space to protect, etc.

For an optical observer, the determined states are the inertial angle pair, α and δ, with the undetermined states as follows

$$\mathbf{x}_d = [\alpha, \delta]^T \tag{38}$$

$$\mathbf{x}_u = [\dot{\alpha}, \dot{\delta}, \rho, \dot{\rho}]^T. \tag{39}$$

Note that while angular rates are not instantaneously observed, they are often inferred from a series of measurements. From a tasking perspective, this paper assumes that regardless of the angular rate of the space object, it can be detected if it is in the field of view. This assumption is good in situations where the angular rates of the hypotheses being

considered to not very dramatically over the field of view. If they do vary dramatically, the expansion of the search set is often prohibitively high for a complete search anyway. Therefore the search set should only exist in angular position space, and $\mathbf{x}_d$ should be defined as such.

The observed part of the measurement space for an optical sensor is just the field of view of the sensor. The observed state space is then fully defined by the state of the observer, $\mathbf{o}, \dot{\mathbf{o}}$, and three angles, $[\alpha_u, \delta_u, \theta_u]$, where α_u and δ_u define pointing and θ_u defines rotation about the line of sight vector. For analytic and computational simplicity, this paper will ignore the bore sight rotation, θ_u. The full observation campaign is represented as a pair of vectors of pointing angles,

$$\mathbf{U} = [\boldsymbol{\alpha}_u, \boldsymbol{\delta}_u] \tag{40}$$

where the entire campaign consists of N observations. This is illustrated in Figure 4. An EOS makes a detection (or does not) by taking a series of images in a certain location in the sky. The time spent attempting a detection at time step k, will be represented by $t_I(t_k)$. Once these series of images have been taken, the EOS slews to a new location. Because every sensor mount is different, an arbitrary function, $f_t(\alpha_1, \delta_1, \alpha_2, \delta_2)$, represents the time it takes a particular sensor to slew from location 1 to location 2.

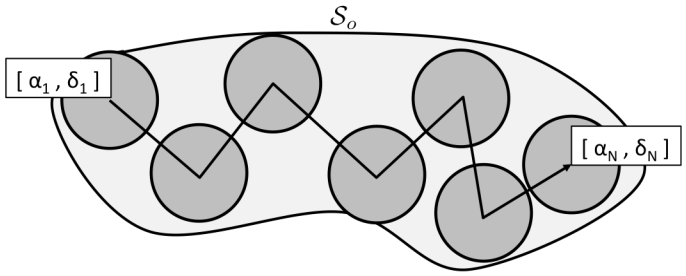

Figure 4. Example of a tasking trajectory over a portion of the sky

If the search set is assumed to be an admissible region, $\mathcal{S} = \mathcal{AR}$, the removal of pieces of search parts of state space can be analytically incorporated into admissible region theory. An admissible region is an intersection of a series of sets, each defined in terms of a constraint,

$$\mathcal{AR} = \bigcap \mathcal{AR}_j \tag{41}$$

$$\mathcal{AR}_j = \{\mathbf{x}_u \in \mathbb{R}^u : g_i(\mathbf{x}_u; \mathbf{x}_d, \dot{\mathbf{x}_d}, \mathbf{k}) \leq 0\} \tag{42}$$

where g_i is a constraint and $\mathbf{k}$ is a parameter vector. The removal of observed parts of state space defines a new admissible region,

$$\mathcal{AR}_j = \{\mathbf{x}_u \in \mathbb{R}^u : \phi(t_k; \mathbf{x}_u, \mathbf{x}_d, t_o) \notin \mathcal{O}(t_k), \forall k\} \tag{43}$$

which in essence removes whatever section(s) of an admissible region that intersect a particular observation.

B. Time Optimal Cost Function

Typically, a search region has positive over all divergence, though there can exist cases where this may not be the case. Regardless, it can be easily checked for a given search region. Time optimal search is built on the assumption that sensor time is a valuable commodity, and the best way to optimally use a sensor is to spend as little time accomplishing a task as possible. The cost function is then the total time spent over the observation campaign,

$$f_{time}(\boldsymbol{\alpha}, \boldsymbol{\delta}) = \sum_{k=1}^{N-1} [t_{I,k} + f_t(\alpha(t_k), \delta(t_k), \alpha(k+1), \delta(k+1))] + t_{I,N} \tag{44}$$

The constraint is difficult to enforce directly as it depends upon the intersection of time varying sets. Instead it can be enforced as a penalty function

$$f_{cost}(\boldsymbol{\alpha}, \boldsymbol{\delta}) = f_{time}(\boldsymbol{\alpha}, \boldsymbol{\delta}) + f_{penalty}(\boldsymbol{\alpha}, \boldsymbol{\delta}; \mathcal{S}) \tag{45}$$

Specifically, this is an exterior penalty function [20]; as the tasking scheme becomes inadmissible, a large cost is added to the function forcing the constraint to be enforced. Penalty functions have a known problem in that they can lead

to inadmissible solutions to the optimization. The penalty function in practice is enforced with a discrete point wise approximation of the search space, $\mathcal{S}(t)$, to approximate the percentage of the set contained in the observation,

$$f_{penalty}(\alpha, \delta; \mathcal{S}) = c\,|\mathcal{S}(t_f)|_{\mathbf{h}} \tag{46}$$

keeping in mind that the search set is reduced in size at every time step, according to Equation (10). The exterior penalty function includes a scaling parameter, c, which is typically increased as iterations of the optimization progress, to better assure the constraint is enforced.

C. Divergence Greedy Cost Function

Because of the computational difficulty of doing a full optimization a second optimization method is being proposed. This method is again based on the idea that search should be done quickly to make best use of a sensor. Furthermore, it is assumed that there is no PDF to define the location of an object, only a set. This is particularly relevant to follow up on an admissible region. Consider Equation (34). At a given time step, k, the best control is the one which minimizes $\mathcal{S}_o(t)$ for all time. This implies that the observed space should be as big as possible, but it also implies the divergence is as big as possible. By maximizing the divergence in the observed space, the rate of change of area at future time steps is minimized. This optimization can be solved at each time step, but is better posed in a finite time horizon manner. Again, assume a series of observations defined in Equation (40), but assume further that the total number of observations, N defines a finite horizon over which the optimizer will search. A cost function which looks to search the largest area possible with the largest divergence possible would then be

$$f_{Div} = -\sum_{k=1}^{N} \frac{\mathrm{d}}{\mathrm{d}t} |\mathcal{O}_o(\mathbf{u}(t_k)) \cap \mathcal{S}_o(t(t_k))| \tag{47}$$

keeping in mind that $\mathcal{S}_o(t_k)$ changes each time step based on both dynamics and sections being removed by previous observations. Note that the total divergence is proportional to the area which is integrated over, so this cost function will prefer large, highly divergent regions.

D. Optimization Methods Tried

This section will discuss a few of the optimization methods attempted on the above problems and report on the success of them.

On the full time optimal cost function, first a basic decent method was tried. The performance of the decent method was well below acceptable, primarily due to two considerations. First, the region itself is highly multi-modal, and fairly poor local optimum are often convergent. Second, the nature of the problem formulation requires a discrete point approximation of the set. The constraint on the optimization, in the form of a penalty function, therefore acts as a step function when calculating the derivatives, making an accurate approximation difficult.

Because a stochastic optimization method is clearly needed, a genetic algorithm was briefly tested. The genetic algorithm proved insufficient, primarily due to the high dimensional nature of the search space and the computational requirements to run a robust enough genetic algorithm on this problem.

Finally a simulated annealing-like algorithm was implemented. Over all, this algorithm had the best success; it was able to search the complicated region, avoid the many local minima, avoid derivatives, and generally behave as a decent method would. Even the success of the simulated annealing was only a partial success. A global minimum is very difficult to find, and stochastic search methods are inherently unrepeatable. The algorithm, after fine tuning, can find an acceptable solution reliably, but often creates obviously suboptimal solutions. More details on this algorithm can be found in [21]. The difficulties of this search method motivated this paper's work on analysis that could inform the search before an optimization take place, and enable a smaller scope optimization like the receding horizon method.

E. Joint Tasking and Estimation of Search Region

This section will discuss related and future work regarding how the above control methods should fit into a broader tasking and estimation framework.

This paragraph will talk about broader tasking schemes in which this algorithm exists. There exist a variety of methods to handle the scheduling problem [3, 4, 5], as discussed in the introduction. These methods can all be used in conjunction with the method described in this paper. A scheduling algorithm can be used to decide between multiple prior distributions and multiple sensors, while the tasking algorithm in this paper prescribes how a sensor searches through a particular prior. Area growth rate estimation can be used as a foundation for a scheduling algorithm, which

is future work from this paper. Finally, it is worth mentioning that scheduling problem is a special case for the work in this paper, and the combined scheduling tasking problem can be considered one problem within the framework of this paper. The computational tractability of this problem, which is in essence a second TSP wrapped around the TSP considered in this paper, is not practical.

This paragraph will talk about estimation schemes which make sense to be used in conjunction with this algorithm. In the case that prior information on a single object is represented with a PDF, a fairly standard Baysian filter is sufficient. This can take the form of a Kalman-like filter, or a non-linear particle or Gaussian mixture filter [9]. Special considerations must be taken in order to account for false and missed detections, if necessary. For operating on an admissible region, there are two primary options. The first method makes a uniform prior distribution assumption and uses Baysian estimation, similar to above [8]. A second newer method exist which makes no uniform prior distribution assumption, instead modeling the set with an uninformative prior and using Dempster-Shafer theory to perform estimation [22]. This method of uninformative priors has not been explicitly extended to a general set for orbit estimation, but such a method should work and would apply to all cases in this paper. Neither of these methods consider how estimation should be handled when a measurement only interrogates a subset of the statespace, rather than the whole space. However, Dempster-Shafer theory's use of belief and plausibility may provide an interesting framework to directly account for partial state space interrogation. This will be a primary area of future work for this paper.

IV. Simulation Test Results

A. Test on Colocated Reacquisition

This test case demonstrates the results of the analytic work and control implementation on a test case with a small size, 2 dimensional manifold This allows the full power of this work to be demonstrated on a best-case, but still useful, scenario. In this test case one observer, located at Georgia Institute of Technology, observes a single unknown space object (Geosynchronous) receiving a short arc observation generating an admissible region. The UTC time is such that the Earth centered earth fixed, and earth centered inertial frames are aligned at $t = 0$, for simplicity.

GS Latitude	GA Longitude	SO $\mathbf{r}$	SO $\dot{\mathbf{r}}$
$33.78°$	$-84.40°$	$[-27.1, -32.3, -0.1]^T \times 10^3$ km	$[2.36, -1.98, 0.0]^T$ km/s

One hour is allowed to pass, and reacquisition is attempted on the space object given the information available in the admissible region.

First, an analysis of the region area as a function of time is presented. The region is propagated over the course of a one hour interval, starting one hour after the first observation is taken. The region after one hour has a size of 0.54 millisteradians, and after two hours has a size of 14 millisteradians. The area is then also predicted out over the same time period using the area time derivatives. Figure 5 presents the true and estimated areas over this hour time period for first through fifth order Taylor series approximation. Percent error can be reduced further with higher order approximations.

Next, an actual observation control trajectory is calculated. As a reminder, a variety of control and optimization algorithms are discussed above. This paper does not spend the time presenting a detailed analysis of the best control algorithm for this problem, and so the results presented here will be of a limited scope. For this test case, a 50 observation time horizon is used to create a 50 observation tasking, using an exhaustive search.

Filed of View width	Staying time at location	Slew time between locations
$0.25°$	15 seconds	0 seconds

The trajectory is calculated for 50 observations over which a majority of the region is observed. Figure 6 shows snapshots of the trajectory after 5, 20, 35, and 50 observations. The black x's are the locations of the various observations. The black square is the current location of the sensor field of view. The region moves in the positive Right Ascension direction, while simultaneously expanding over the course of the simulation. The optimal trajectory tends to move in the negative right ascension direction, against the movement of the region. Because of these movements in opposite directions, the trajectory appears to dwell in the same area for an extended period of time, but the observations are all looking at a completely new area in the set. Figure 7 shows the area of the original region, and the area of the unobserved region over time. The figure illustrates the difficulty of this test case; the original region is growing at a substantial rate, which is constantly fighting against the observation schemes ability to scan the region.

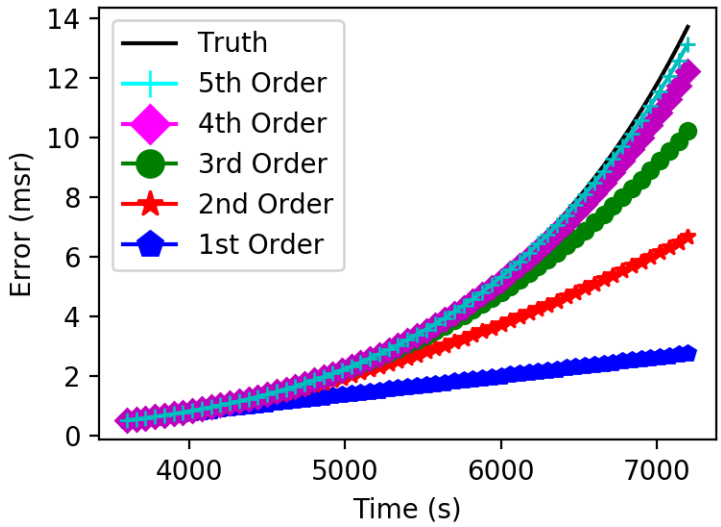

Figure 5. Absolute error for various Talyor series area approximations.

B. Validation of Telescope System

In order to test the validity of the methods in this paper, a scenario similar to the above is demonstrated on a the Georgia Tech Space Object Research Telescope.

The object cluster around the EchoStar 16 satellite is fictitiously observed at UTC $= [2017, 09, 07, 02, 15, 00]$, or 10:15pm local time on September 6th, in Atlanta. Reacquisition was attempted at UTC $= [2017, 09, 07, 03, 00, 00]$, or 11:00pm local time on September 6th, in Atlanta. The calculated trajectory is show in Figure 8. At the second tasking location, 5 images were taken, one of which is shown in Figure 9. The tasking tracked a given right ascension and declination, so stars appear stationary while space objects appear to streak. Three objects in the cluster are highlighted on the image.

C. Test on Geostationary Slot Protection

The final test case demonstrates the method operating on a more complicated set. This set is defined as the objects in a geostationary transfer orbit (GTO), which reach apoapse in a particular geostationary slot. Specifically, the radius of periapse is set as constant, the position at apoapse is any where in a cube of 73 km sides centered around a geostationary object, approximating a "GEO slot", the inclination is between -5 and +5 degrees, and the time until intercepting GEO is between 10 and 40 minutes. Note that the above definition uses negative inclination to represent objects coming up from below the GEO plane (e.g. $i = -5$ is really an $i = +5$ but with true anomaly, argument of perigee, and argument of ascending node rotated by $180°$).

The resulting region is a trapazoidal set of orbits which get closer together as they approach the target GEO slot. The exact same method is used to calculate a trajectory to scan through the region with, which is shown in Figure 10. Because of the nature of this set, it is actually getting smaller as time goes on meaning the area rate is negative. The total area and unobserved area are shown in Figure 11.

V. Conclusion

A. Intuitive Concepts and Conclusions

This paper provides a framework for SSA tasking strategies. Reacquisition, scheduling, custody, and search operations can all be represented with a search set. As such, all can be analyze with the divergence methods presented in this paper.

A search set is best analyzed when projected into the measurement space of a particular observer. The evolution of these regions over time is dominated by the vector field of velocity and higher order derivatives and the divergence of those vector fields, along the boundary of the search set. This allows quick analytic solutions for the evolution of the

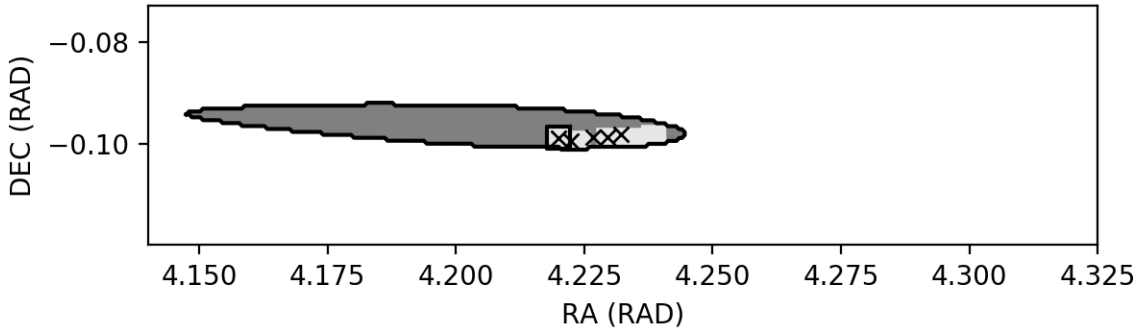

a) Trajectory after 5 Observations.

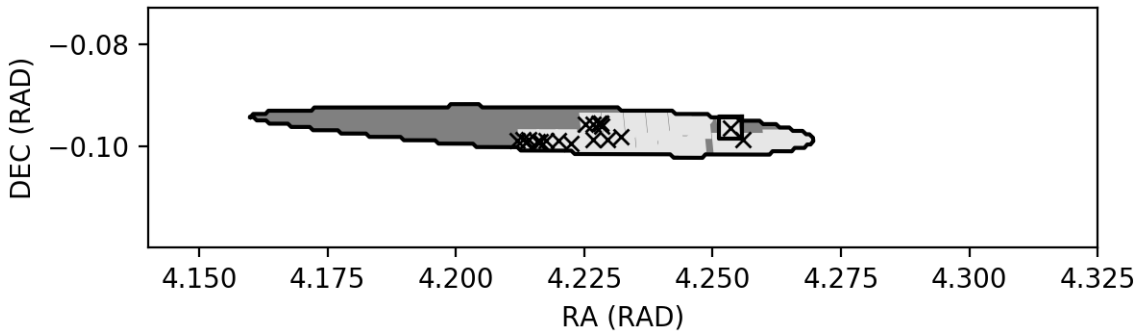

b) Trajectory after 20 Observations.

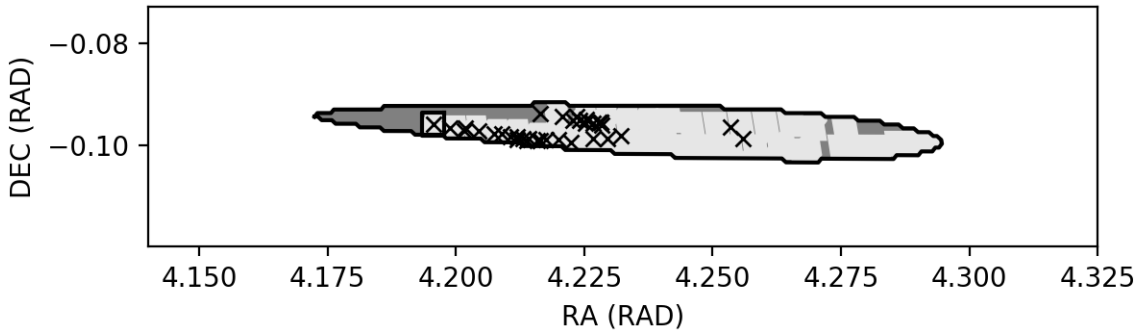

c) Trajectory after 35 Observations.

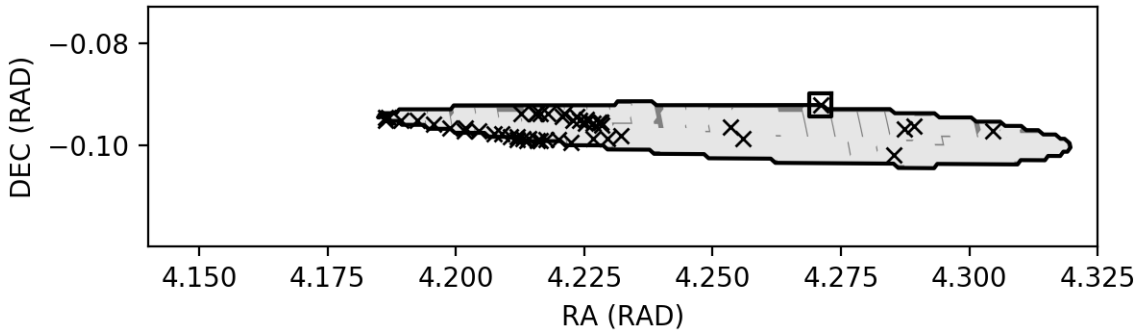

d) Trajectory after 50 Observations.

Figure 6. Same location hand-off results.

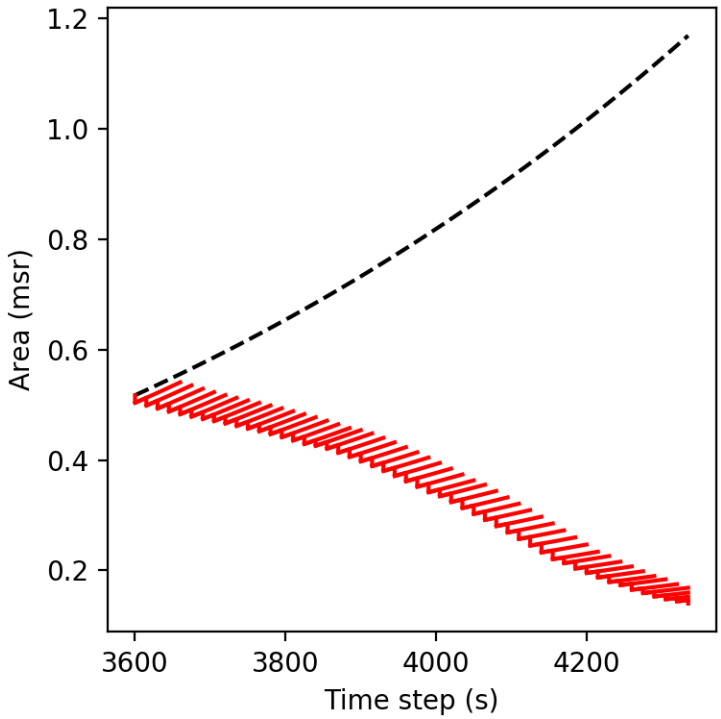

Figure 7. Total area and observed area over time.

search set over time. The area over time makes for a suitable metric for both analyzing and predicting tasking schemes on a search set. This metric also is suitable for use as a control scheme cost function.

B. Limitations of Method

Many search sets are still infeasible to search, and this method does little to solve that problem. Rather, it provides tools to analyze search sets, and show how to make search feasible. This will not always be easy or possible.

Search sets can be tricky to define in a clean analytic way, making the clean analytic equations involved in this paper difficult to calculate. Non-injective measurement functions are possible to work with, but make analysis more difficult and less meaningful.

C. Opportunities for Future Work

Area over time is a simplistic bulk measure for search sets. One area of future work should be to provide more complex predictions which better take into account search space shape and how it will intersect with sensor field of view. If such an analysis can be worked into a cost function, it will create a powerful optimization tool. Sensor design is an obvious extension of this work. The analysis provided take both sensor location and sensor parameters into consideration, and the analysis can be easily turned around to look at what those factors should be to provide certain search capabilities. The actual estimation of objects which exist in a set may prove to be more complicated than one might think. Methods based on finite set statistics and Dempster Shaffer belief ignorance theory may provide the best avenue. Such a method should allow for a solution of no objects, one object, or many objects existing in the set.

VI. Acknowledgment

This research was conducted with Government support under and awarded by DoD, Air Force Office of Scientific Research, National Defense Science and Engineering Graduate (NDSEG) Fellowship, 32 CFR 168a. I would like to personally thank Chris Sabol, Kim Luu, and Brien Flewelling for their guidance and inspiration throughout my graduate school career. We would like to acknowledge and thank the Air Force Research Laboratory Scholars Program

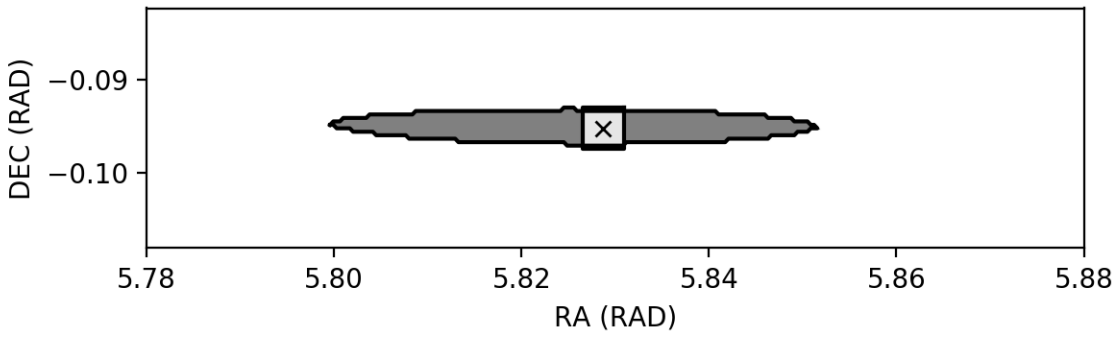

a) Trajectory after 1 Observations.

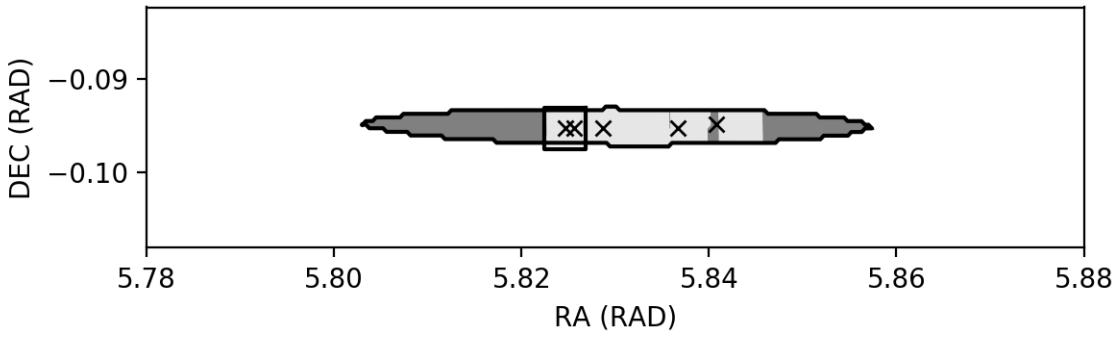

b) Trajectory after 5 Observations.

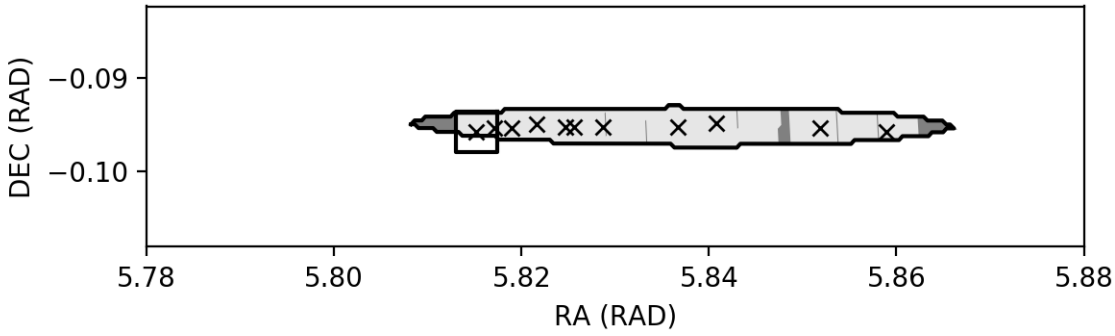

c) Trajectory after 10 Observations.

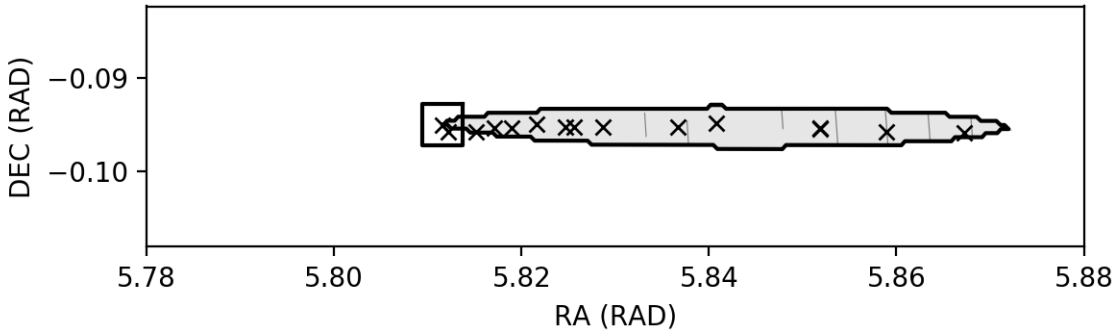

d) Trajectory after 15 Observations.

Figure 8. Calculated Trajectory

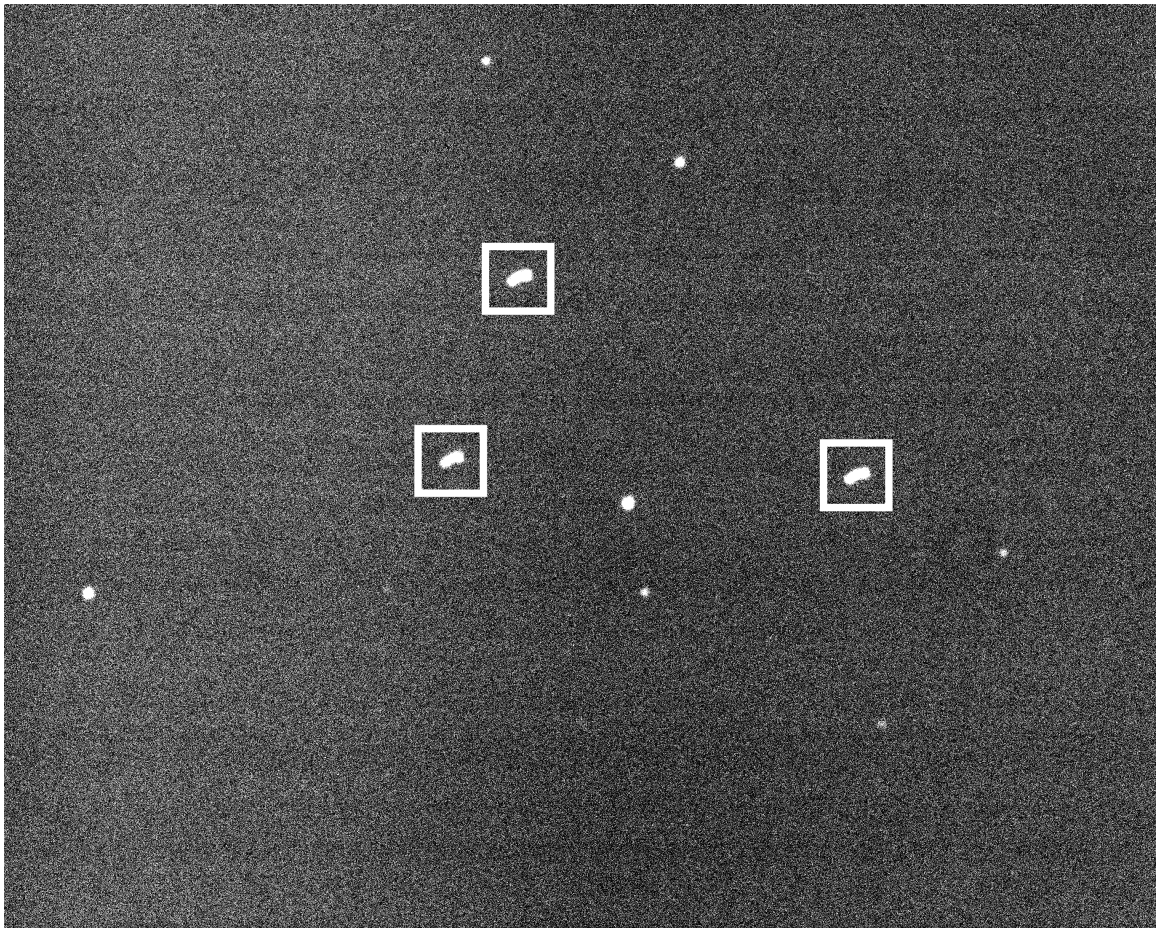

Figure 9. Image of ECHOSTAR 16 Object Cluster

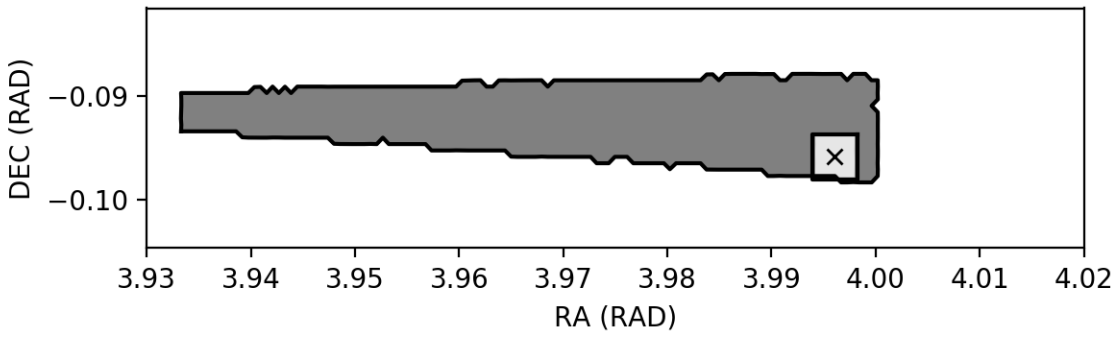

a) Trajectory after 5 Observations.

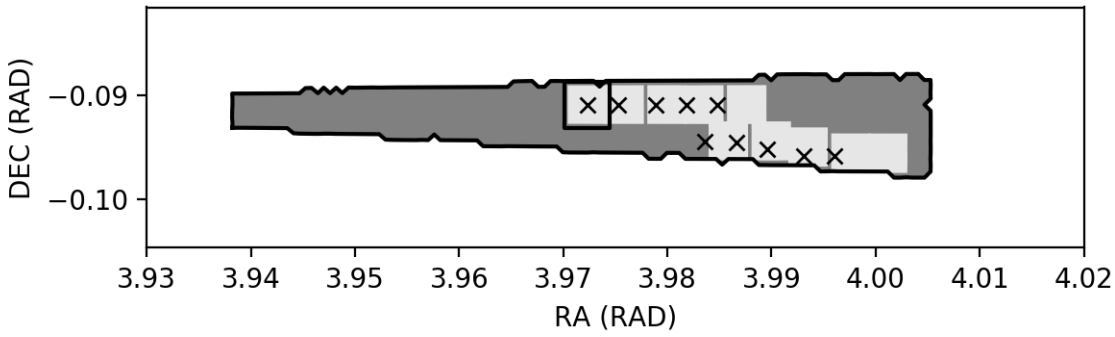

b) Trajectory after 20 Observations.

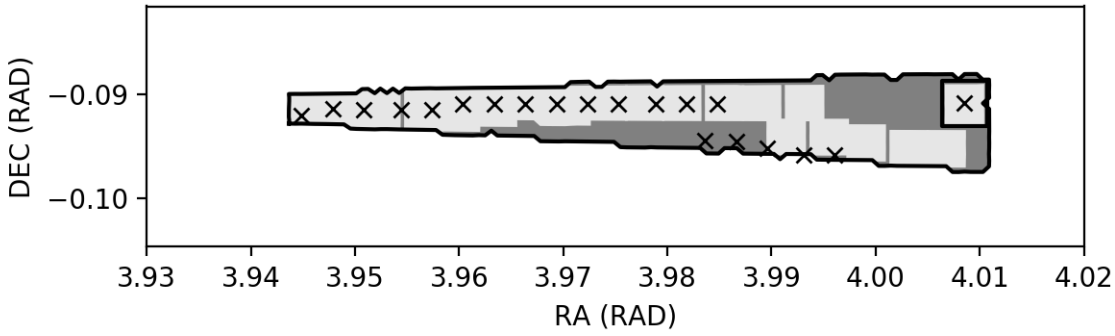

c) Trajectory after 35 Observations.

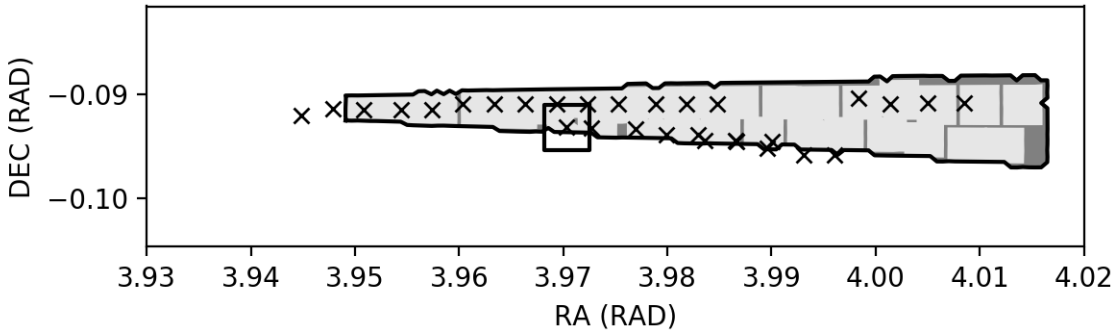

d) Trajectory after 50 Observations.

Figure 10. Same location hand-off results.

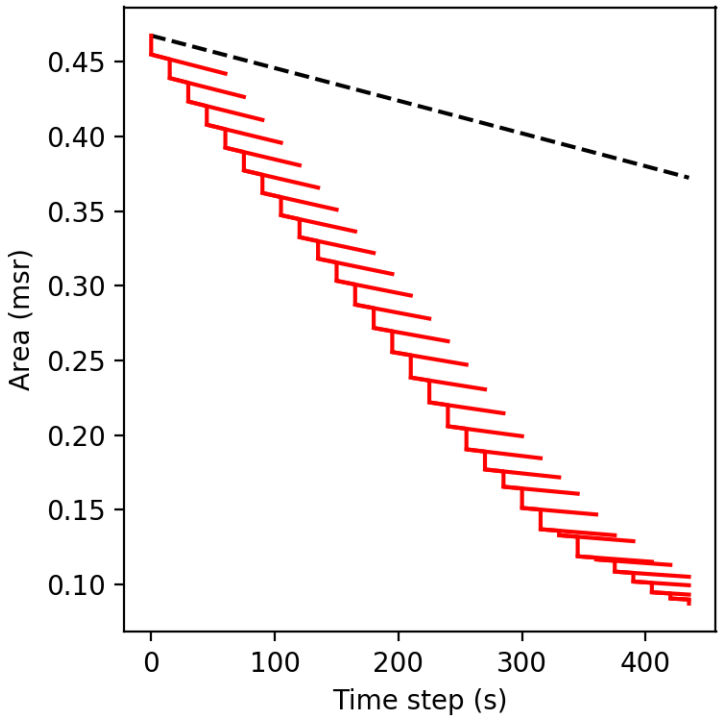

Figure 11. Total area and observed area over time.

for supporting this project. Finally, Dr. Ryan Coder, Andris Jaunzemis, Shez Virani, Daniel Aguilar and all past and future contributors to GT-SORT and SSA.py.

VII. Appendix I: Higher Order Derivatives

In order to accurately project area of a region forward in time, higher order derivatives should be used in the Taylor series expansion. Below are the derivatives of area from the first to the fifth time derivative. The general form is identical to higher order time derivatives of $f(t) = x(t) \cdot y(t)$, where $x(t)$ is $\dot{\mathbf{x}}_d$ and $y(t)$ is $\frac{\partial \mathbf{x}_d}{\partial \mathbf{x}_d}$

$$\frac{\mathrm{d}}{\mathrm{d}t} A_{\mathbf{h}}(\mathcal{S}) = \oint_{\partial \mathcal{S}_d} (\dot{\mathbf{x}}_d \cdot \hat{\mathbf{n}}) \mathrm{d}S \tag{48}$$

$$\frac{\mathrm{d}^2}{\mathrm{d}^2 t} A_{\mathbf{h}}(\mathcal{S}) = \oint_{\partial \mathcal{S}_d} \left(\ddot{\mathbf{x}}_d + \dot{\mathbf{x}}_d \cdot \frac{\partial \dot{\mathbf{x}}_d}{\partial \mathbf{x}_d} \right) \cdot \hat{\mathbf{n}} \mathrm{d}S \tag{49}$$

$$\frac{\mathrm{d}^3}{\mathrm{d}^3 t} A_{\mathbf{h}}(\mathcal{S}) = \oint_{\partial \mathcal{S}_d} \left(\dddot{\mathbf{x}}_d + 2\ddot{\mathbf{x}}_d \cdot \frac{\partial \dot{\mathbf{x}}_d}{\partial \mathbf{x}_d} + \dot{\mathbf{x}}_d \cdot \frac{\partial \ddot{\mathbf{x}}_d}{\partial \mathbf{x}_d} \right) \cdot \hat{\mathbf{n}} \mathrm{d}S \tag{50}$$

$$\frac{\mathrm{d}^4}{\mathrm{d}^4 t} A_{\mathbf{h}}(\mathcal{S}) = \oint_{\partial \mathcal{S}_d} \left(\ddddot{\mathbf{x}}_d + 3\dddot{\mathbf{x}}_d \cdot \frac{\partial \dot{\mathbf{x}}_d}{\partial \mathbf{x}_d} + 3\ddot{\mathbf{x}}_d \cdot \frac{\partial \ddot{\mathbf{x}}_d}{\partial \mathbf{x}_d} + \dot{\mathbf{x}}_d \cdot \frac{\partial \dddot{\mathbf{x}}_d}{\partial \mathbf{x}_d} \right) \cdot \hat{\mathbf{n}} \mathrm{d}S \tag{51}$$

$$\frac{\mathrm{d}^5}{\mathrm{d}^5 t} A_{\mathbf{h}}(\mathcal{S}) = \oint_{\partial \mathcal{S}_d} \left(\dddddot{\mathbf{x}}_d + 4\ddddot{\mathbf{x}}_d \cdot \frac{\partial \dot{\mathbf{x}}_d}{\partial \mathbf{x}_d} + 6\dddot{\mathbf{x}}_d \cdot \frac{\partial \ddot{\mathbf{x}}_d}{\partial \mathbf{x}_d} + 4\ddot{\mathbf{x}}_d \cdot \frac{\partial \dddot{\mathbf{x}}_d}{\partial \mathbf{x}_d} + \dot{\mathbf{x}}_d \cdot \frac{\partial \ddddot{\mathbf{x}}_d}{\partial \mathbf{x}_d} \right) \cdot \hat{\mathbf{n}} \mathrm{d}S \tag{52}$$

This gives a general formula for the nth derivative.

$$\frac{\mathrm{d}^n}{\mathrm{d}^n t} A_{\mathbf{h}}(\mathcal{S}) = \oint_{\partial \mathcal{S}_d} \sum_{i=1}^{n} \mathbf{x}_d^{(i)} \cdot \frac{\partial \mathbf{x}_d^{(n-i)}}{\partial \mathbf{x}_d} \tag{53}$$

References

[1] Blake, T., Sánchez, M., Krassner, J., Georgen, M., and Sundbeck, S., "Space Domain Awareness," *Advanced Maui Optical and Space Surveillance Technical Conference*, 2011.

[2] Abdelkhalik, O. O., Mortari, D., and Junkins, J. L., "Space surveillance with star trackers. Part ii: Orbit estimation," *Space Flight Mechanics Meeting Conference*, 2006.

[3] Erwin, R. S., Albuquerque, P., Jayaweera, S. K., and Hussein, I., "Dynamic sensor tasking for Space Situational Awareness," *Proceedings of the 2010 American Control Conference*, Institute of Electrical & Electronics Engineers (IEEE), jun 2010. doi:10.1109/acc.2010.5530989.

[4] Sunberg, Z., Chakravorty, S., and Erwin, R., "Information space sensor tasking for Space Situational Awareness," *2014 American Control Conference*, Institute of Electrical and Electronics Engineers (IEEE), jun 2014. doi:10.1109/acc.2014.6858922.

[5] Jaunzemis, A., Holzinger, M., and Jah, M., "Evidence-based Sensor Tasking for Space Domain Awareness," *Advanced Maui Optical and Space Surveillance Technologies Conference*, 2016.

[6] Gehly, S., Jones, B., and Axelrad, P., "Sensor Allocation for Tracking Geosynchronous Space Objects," *Journal of Guidance, Control, and Dynamics*, aug 2016, pp. 0–0. doi:10.2514/1.g000421.

[7] Hobson, T. A. and Clarkson, I. V. L., "A particle-based search strategy for improved Space Situational Awareness," *2013 Asilomar Conference on Signals, Systems and Computers*, Institute of Electrical & Electronics Engineers (IEEE), nov 2013. doi:10.1109/acssc.2013.6810418.

[8] DeMars, K. J., Jah, M. K., and Schumacher, P. W., "Initial orbit determination using short-arc angle and angle rate data," *Aerospace and Electronic Systems, IEEE Transactions on*, Vol. 48, No. 3, 2012, pp. 2628–2637.

[9] DeMars, K. J. and Jah, M. K., "Probabilistic initial orbit determination using gaussian mixture models," *Journal of Guidance, Control, and Dynamics*, Vol. 36, No. 5, 2013, pp. 1324–1335.

[10] Milani, A., Gronchi, G. F., Vitturi, M. d., and Knežević, Z., "Orbit determination with very short arcs. I admissible regions," *Celestial Mechanics and Dynamical Astronomy*, Vol. 90, No. 1-2, 2004, pp. 57–85.

[11] Worthy III, J. L. and Holzinger, M. J., "Incorporating Uncertainty in Admissible Regions for Uncorrelated Detections," *Journal of Guidance, Control, and Dynamics*, Vol. 0, No. 0, 2015, pp. 1–17. doi:10.2514/1.g000890.

[12] Hobson, T., Clarkson, I., Bessell, T., Rutten, M., Gordon, N., Moretti, N., and Morreale, B., "Catalogue Creation for Space Situational Awareness with Optical Sensors," *Advanced Maui Optical and Space Surveillance Technologies Conference*, 2016.

[13] Hobson, T., Gordon, N., Clarkson, I., Rutten, M., and Bessell, T., "Dynamic steering for improved sensor autonomy and catalogue maintenance," *Advanced Maui Optical and Space Surveillance Technologies Conference, Wailea, HI*, 2014.

[14] Gutin, G. and Punnen, A. P., editors, *The Traveling Salesman Problem and Its Variations*, Springer US, 2007. doi:10.1007/b101971.

[15] Worthy III, J. L., Holzinger, M. J., and Scheere, D. J., "An Optimization Based Approach to Corellation of Observations with Uncertainty," *AIAA/AAS Space Flight Mechanics Conference*, 2016.

[16] Sease, B., Schmittle, K., and Flewelling, B., "MULTI-OBSERVER RESIDENT SPACE OBJECT DISCRIMINATION AND RANGING," *AAS/AIAA Space Flight Mechanics Meeting*, 2015.

[17] Holzinger, M. J., Scheeres, D. J., and Alfriend, K. T., "Object Correlation, Maneuver Detection, and Characterization Using Control Distance Metrics," *Journal of Guidance, Control, and Dynamics*, Vol. 35, No. 4, jul 2012, pp. 1312–1325. doi:10.2514/1.53245.

[18] Kirkpatrick, S., Gelatt, C. D., and Vecchi, M. P., "Optimization by Simulated Annealing," *Science*, Vol. 220, No. 4598, may 1983, pp. 671–680. doi:10.1126/science.220.4598.671.

[19] Chavel, I., *Riemannian Geometry*, Cambridge University Press, 2006. doi:10.1017/cbo9780511616822.

[20] Vanderplaats, G. N., "Multidiscipline Design Optimization," *Applied Mechanics Reviews*, Vol. 41, No. 6, jun 1988, pp. 257. doi:10.1115/1.3151897.

[21] Murphy, T. S., Holzinger, M. J., Luu, K. K., and Sabol, C., "Optical Sensor Follow-Up Tasking on High Priority Uncorrelated Track," *AAS/AIAA Space Flight Mechanics Meeting*, 2017.

[22] Worthy III, J. L. and Holzinger, M. J., "Dempster-Shafer Theory Applied to Admissible Regions," *AIAA/AAS Space Flight Mechanics Conference*, 2017.